Measurement of bacterial size via image analysis of epifluorescence preparations: description of an inexpensive system and solutions to some of the most common problems*

RAMON MASSANA[1], JOSEP M. GASOL[1], PETER K. BJØRNSEN[2], NICHOLAS BLACK-BURN[3], ÅKE HAGSTRÖM[4], SUSANNA HIETANEN[5], BENT H. HYGUM[4], JORMA KUPARINEN[5] and CARLOS PEDRÓS-ALIÓ[1]

[1]Institut de Ciències del Mar, CSIC. Passeig Joan de Borbó, s/n. E-08039 Barcelona, Spain. Phone: 343 - 221 6416. Fax: 343- 221 7340. E-mail: ramonm@icm.csic.es
[2]University of Copenhagen. Marine Biological Laboratory. Strandpromenaden 5. DK-3000 Helsingør, Denmark.
[3]University of Umeå, Department of Microbiology, Marine Center, S-91020 Hönefors, Sweden.
[4]National Environmental Research Institute. Department of Marine Ecology and Microbiology. DK-4000 Roskilde, Denmark.
[5]Finnish Institute of Marine Research, P.O.Box 33, FIN-00931 Helsinki, Finland.

SUMMARY: Computerized image-analysis of epifluorescence preparations is the most accurate and simple method for the estimation of bacterial size. We present a simple and inexpensive image-analysis system used to measure and count planktonic bacteria and presently in operation in our laboratory. We show that there is a wide range of image exposures (brightness) over which the system performs correctly. Even though the procedure involves some steps that depend upon operator intervention, the results obtained are highly reproducible and we have estimated the among-operator variability at 5%. We then discuss the advantages and disadvantages of different algorithms used for the estimation of volume from two-dimensional images and we identify those that perform better for curved and unusual cells. We finally estimate that 4 to 6 images and 200 - 250 cells are the optimal number of images to be processed and cells to be measured to obtain accurate estimates of population values with the minimum effort. These calibrations should be useful to all those laboratories that are implementing image-analysis systems.

Key words: Bacterial size, image analysis, epifluorescence microscopy.

RESUMEN: El análisis de imágenes obtenidas a partir de preparaciones de epifluorescencia es el método más sencillo y preciso para medir el tamaño bacteriano. En este trabajo se presenta un sistema de análisis de imágenes sencillo y asequible, actualmente en funcionamiento en nuestro laboratorio, desarrollado para medir y contar bacterias planctónicas. Se demuestra que el sistema funciona correctamente dentro de un rango amplio de brillo de imagen. Aunque algunos pasos del proceso dependen del operador, los resultados obtenidos fueron altamente reproducibles, y se estimó una variabilidad entre operadores del 5%. Se discuten las ventajas de los diferentes algoritmos usados para calcular el biovolumen a partir de imágenes de dos dimensiones, e identificamos el algoritmo que funciona mejor en células curvados o de formas inusuales. Finalmente, se estimó que para obtener medidas precisas del tamaño medio de la población con el mínimo esfuerzo se debían procesar entre 4 y 6 imágenes y contar entre 200 y 250 células. La información presentada en este trabajo puede ser útil para aquellos laboratorios que deseen desarrollar sistemas de análisis de imágenes parecidos.

Palabras clave: Tamaño de bacterias, análisis de imágenes, microscopía de epifluerescencia.

INTRODUCTION

Size of an organism is an ecologically important factor because it determines many aspects of its metabolism, food size range and susceptibility to predators (Peters, 1983). Thus, size can be used to define individual and population characteristics of groups of organisms. Size is also a factor required for converting concentrations of organisms to biomass, a value necessary to assess the role of the organisms in the carbon cycle. For the smallest organisms of the plankton, prokaryotes and small eukaryotes, size is a parameter easier to determine than genetic identity, and size diversity has been proposed as a method to characterize picoplanktonic communities (Gasol *et al.*, in press).

Even though size of planktonic bacteria is sometimes taken as a constant, it is well known that it changes with growth rate (Chrzanowski *et al.*, 1987; Bjørnsen *et al.*, 1989; White *et al.*, 1991), temperature (Chrzanowski *et al.*, 1987), activity (Gasol *et al.*, 1995), nutrient availability (Billen *et al.*, 1990) or grazing pressure (Jürgens and Güde, 1994). Certain cells can be very large in nature (Cole *et al.*, 1993; Sommaruga and Psenner, 1995), while starved cells are commonly very small (Novitsky and Morita, 1976). In a given system, the ratio between the smallest cell and the biggest one can be as high as 100 (Cole *et al.*, 1993). Considering the average for the community, cell size can vary from 0.03 μm^3 in an Antarctic open-ocean sample (Lee *et al.*, 1995) to more than 1 μm^3 in marine snow bacteria (Alldredge *et al.*, 1986). Average bacterial size is, thus, an important parameter that can provide ecologically important information about the bacterial assemblage.

Several methods have been used in the past to estimate average bacterial size: electron microscopy, electronic devices (Coulter counter and flow cytometry), and epifluorescence microscopy. Transmission electron microscopy is tedious and expensive because samples require long and elaborate processing before analysis. Scanning electron microscopy is relatively faster and cheaper, but processing of the samples may produce cell shrinkage and underestimation of bacterial size (Fuhrman, 1981). Coulter counters have a very low resolution in the bacterial size range and do not discriminate between bacteria and dead or inert particles. Flow cytometry has similar limitations, although specific staining may solve some of these problems (Robertson and Button, 1989; Li *et al.*, 1995; del Giorgio *et al.*, 1996). The most popular method for bacterial size measurement relies on epifluorescence images of DAPI, Acridine Orange or Acriflavine stained bacteria. Direct sizing with a calibrated eyepiece is time-consuming (one cell at a time) and not very precise. Obtaining a photograph from the sample, projecting it and measuring the bacteria on a screen introduces an additional step in the procedure and is also time consuming. Direct computerized image analysis of the epifluorescence samples is the most precise and fastest method, as long as procedures are developed for cell edge detection and for converting cell area to volume.

There are several papers describing the development of image analysis systems used to measure bacterial size. Sieracki *et al.* (1985), Estep *et al.* (1986) and Bjørnsen (1986) were the first to introduce image analysis of epifluorescence images to size bacteria, but the computers and cameras at the time were slow and expensive. Sieracki *et al.*
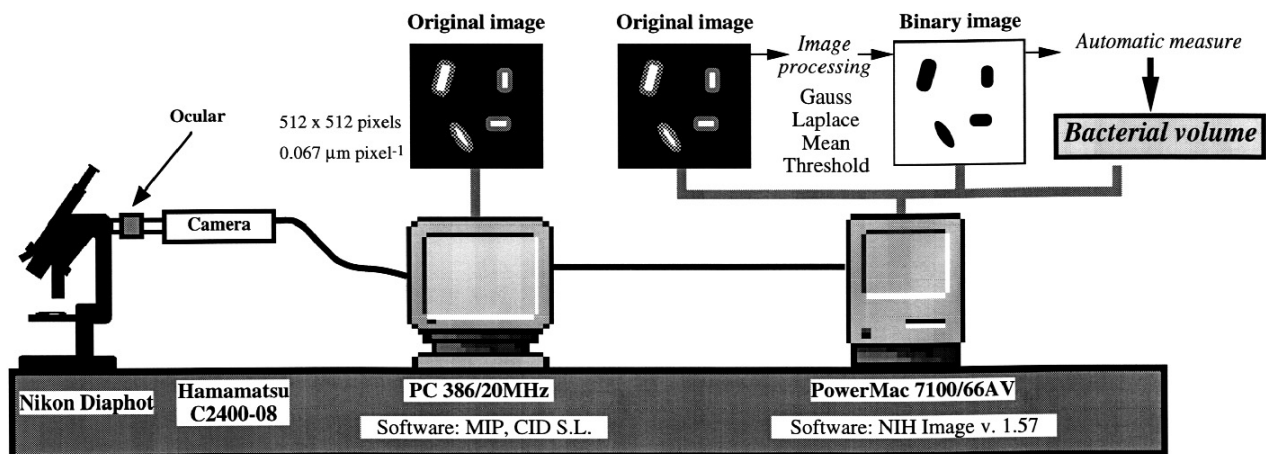

FIG. 1. – Schematic presentation of the hardware and the image analysis procedure as it is performed in our laboratory.

(1989a) proposed a method of automatic thresholding while Krambeck et al. (1990) suggested a way to solve the halo effects via the application of a nonlinear function. Sieracki *et al*. (1989b) introduced an algorithm to compute biovolume by automatically slicing the cells and rotating each slice. A review of the method, with many useful suggestions can be found in Psenner (1993). More recently, newer and more sophisticated systems have been introduced: cooled charge-coupled cameras (Viles and Sieracki, 1992), color cameras (Sieracki and Webb, 1991; Verity and Sieracki, 1993), or even digital confocal laser microscopy, a very sophisticated method that can reach precisions of 0.049 μm pixel[-1] (Bloem *et al*., 1995). However, most of these systems are relatively inaccessible to most researchers, specially due to the prices.

In this paper we present a simple image-analysis system, describing the whole process from sample preparation to volume determination. Since many details of image processing have been dealt with in others papers, or are described in unpublished reports, we will cite them without discussion. We will focus on some problems that we have encountered and some of the solutions we have chosen. In our experience, the system we present can be a great aid for other laboratories when trying to setup an image-analysis system.

DESCRIPTION OF THE IMAGE ANALYSIS SYSTEM

Equipment: Hardware and software

The elements required for image analysis of bacterial assemblages are an epifluorescence microscope, a video camera and a computer equipped with video acquisition capabilities (frame grabber) plus the appropriate software for image processing. Our system is slightly more complex because image acquisition and image processing are performed in different computers (Fig. 1), but there is no need for doing so. We use a Nikon Diaphot inverted epifluorescence microscope and a Hamamatsu C2400-08 video camera with a SIT (Silicon-Intensified Target) to amplify the light signal. In the microscope, we introduced a lens (a conventional ocular) in the optical path to the camera, resulting in a pixel size (100x objective) of 0.067 μm pixel[-1]. This value is slightly

lower than that obtained by Psenner (1991, 0.083 μm^{-1} pixel) and Schröder and Krambeck (1991, 0.090 μm pixel[-1]), and identical to that obtained by Hygum (1995) and Sieracki *et al*. (1995) with different image analysis systems. The images are captured by a Mitsubishi 386 PC computer running at 20 MHz, using the commercial software MIP, developed by CID S.L., España. Images have 512 x 512 pixels and 8-bit dynamic range (256 gray levels). The images are downloaded to an Apple Power Macintosh (7100/66) where they are processed with the public domain software NIH-Image v. 1.57 (for powerpc) from the National Institutes of Health, USA, distributed at http://rsb.info.nih.gov/nih-image/. Many different system configurations can be used instead of the one we describe here. A detailed discussion on different image analysis systems and advances using CCD cameras can be found in Verity and Sieracki (1993).

Sample preparation

Water samples are fixed with formaldehyde (2% final concentration) and kept cool and in the dark until processed. Bacteria are stained with DAPI (Porter and Feig, 1980) and collected on 0.2 μm black Nuclepore filters. Other fluorescent dyes could be used as well. High quality images (bright cells and dark background) are necessary for image analysis. The volume of sample to be filtered should be adjusted to maximize the number of bacteria per image without overlapped cells. According to our experience, around 50 cells per image would be optimal. Considering an effective diameter of 16 mm onto which the sample is filtered, and that each image corresponds to an area of 0.12 mm² (34 x 34 μm), this implies the filtration of 8.5 ml of a sample at 10^6 cells ml^{-1}.

Image capture

With the appropriate set up of the microscope, camera and computer, the microscopic fields are directly visualized on the computer screen. Images of very flat fields with enough bacteria and absence of very bright particles are selected to be digitized. The camera controls allow regulation of light intensity so that the bacteria appear as bright as possible without having been overexposed. As we will show later, there is a reasonable range of light intensities that produce similar estimates.
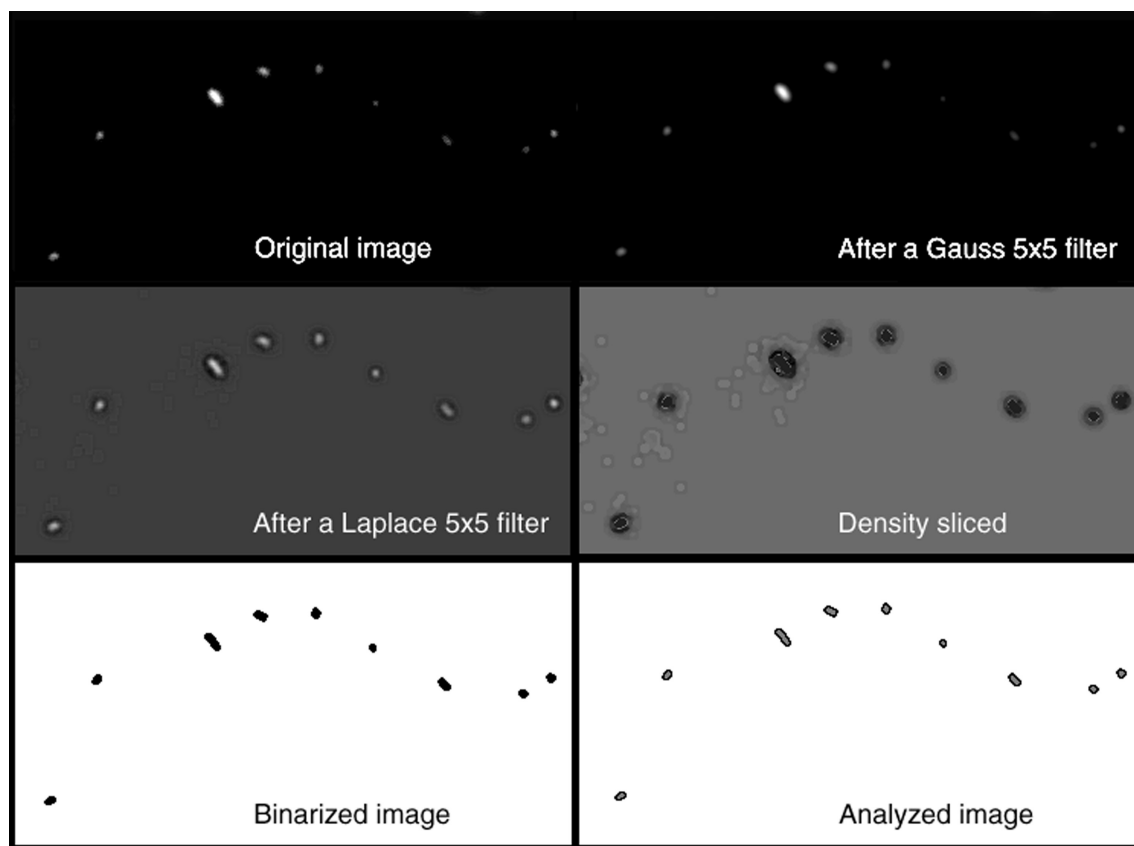
FIG. 2. – Overview of the whole process of image processing. The original image (upper left), is treated with a Gauss filter (upper right) that prepares it for a Laplace filter (middle left). The image is then manually thresholded (middle right) and binarized (lower left). Finally, the program analyzes all the detected objects (lower right).

Image processing

Bacteria visualized through epifluorescence appear as bright objects surrounded by a halo of decreasing light (Psenner, 1991). Because of this, the detection of their edges is not trivial and requires the application of several filters (discussed in detail in Bjørnsen *et al*., 1995). The most important is a second derivative filter (i.e. Laplace) which finds the points of maximal gray level gradient, assumed to coincide with the true edge of bacteria. In addition, other filters must be applied to reduce the noise. We have arrived at an optimal sequence for our system involving the application of a Gauss filter (kernel 5x5), a Laplace filter (kernel 5x5), and a median filter (rank 3), the latter run three times. When working with NIH-Image, the option "Scale Convolutions" should be selected when running the Laplace filter (see later).

After filtering the image, the gray levels corresponding to bacteria are selected in order to obtain the binary image (black particles onto a white back-

ground). This process is done interactively and the criterion is to obtain the biggest cells without selecting non-bacterial objects. As we will discuss latter, the Laplace filter prepares the image in a way that this choice is highly reproducible. Next, the undesirable objects are interactively removed by comparing the binary image with the original one. Finally, the parameters of interest (i.e. Area, Perimeter, Length and Width) are automatically measured for each single bacteria. We decided not to consider particles smaller than 0.2 μm of equivalent diameter, corresponding to the filter pore-size used. Fig. 2 shows the changes in the image throughout the different steps of the process.

Most of the process can be automated by running several Pascal macros that control the software. We routinely apply three scripts, interrupted by the two processes that require operator intervention: choice of the threshold level, and deletion of undesired objects. The macros are available via anonymous FTP at cucafera.icm.csic.es, in the directory pub/Massana.

Algorithm 1. Uses L and W.

Eq. (1)

$$V_1 = \frac{\pi}{4} W^2 \left(L - \frac{W}{3} \right)$$

Algorithm 2. Uses A and L.

Eq. (2)

$$W_e = \frac{2}{(\pi - 4)} \left(\sqrt{L^2 + (\pi - 4)A} - L \right)$$

Eq. (3)

$$V_2 = \frac{\pi}{4} W_e^2 \left(L - \frac{W_e}{3} \right)$$

Algorithm 3. Uses A and P.

Eq. (4)

$$W_e = \frac{P - \sqrt{P^2 - 4\pi A}}{\pi}$$

Eq. (5)

$$L_e = \frac{P}{2} + W_e \left(1 - \frac{\pi}{2} \right)$$

Eq. (6)

$$V_3 = \frac{\pi}{4} W_e^2 \left(L_e - \frac{W_e}{3} \right)$$

Eq. (7)

$$V_4 = \frac{4}{3} \sqrt{\frac{A^3}{\pi}}$$

FIG. 3. – Set of algorithms used to calculate bacterial volume (V) from the parameters obtained by image analysis: Length (L), Width (W), Area (A) and Perimeter (P).

Volume calculations

To calculate a three-dimensional parameter, volume, from the two-dimensional parameters obtained by image analysis, we consider all bacteria to be cylinders with two hemispherical caps. Assuming this model, we present three sets of equations (algorithms) to calculate the volume (Fig. 3). The first one uses directly the Length and Width as read by the software (Eq. 1). The second algorithm uses Area and Length, computing first the equivalent width (Eq. 2) and then the volume (Eq. 3). The third algorithm (Fry 1990) uses Area and Perimeter to compute equivalent width (Eq. 4) and equivalent length (Eq. 5) and then the volume (Eq. 6). We are currently using this third algorithm since it appears to be appropriate for most types of bacteria (see later). This equation, however, caused problems with some very small and round-like cells. In these cases, we calculated the volume using only the Area, and assuming the cell to be a sphere (Eq. 7).

TABLE 1. – Average bacterial volume (SE shown between parenthesis) and bacterial abundance in the samples used for the different calibrations reported in this paper.

System	Average volume (μm^3)	Abundance (cells ml^{-1})
Mediterranean (cruise VARIMED'93)	0.054 (0.003)	1.94 x 10^5
Mediterranean (Blanes Bay)	0.055 (0.001)	8.70 x 10^5
Drake Passage (cruise ECOANTAR'94)	0.040 (0.003)	3.23 x 10^5
Santa Pola salterns (Alicante)		
38 ‰	0.084 (0.004)	9.83 x 10^6
150 ‰	0.106 (0.005)	5.43 x 10^7
352 ‰	0.916 (0.085)	6.47 x 10^7
Lake Redó (Catalonia)	0.116 (0.043)	2.96 x 10^5
Lake Ció (Catalonia)		
Epilimnion	0.058 (0.005)	6.30 x 10^6
Metalimnion	0.104 (0.011)	1.95 x 10^7
Hypolimnion	0.134 (0.015)	1.09 x 10^7
Lake Bowker (Québec)	0.086 (0.004)	3.08 x 10^6
Lake Massawippi (Québec)	0.116 (0.007)	1.40 x 10^6
Lake Waterloo (Québec)	0.063 (0.003)	6.45 x 10^6

Test images

Samples for the different tests and comparisons were taken from several aquatic systems (Table 1), mainly marine environments (FRONTS and VARIMED cruises in the Northwestern Mediterranean and ECOANTAR in the Drake Passage, Weddell Sea and Bransfield Strait in Antarctica), solar salterns (Bras-del-Port, Santa Pola, Southeastern Spain) and freshwater lakes (different lakes in Quebec, the Pyrenees and the Banyoles area, Catalonia). The images used for the interuser comparison reported in Table 2 can be obtained via anonymous FTP at cucafera.icm.csic.es, in the directory pub/Massana.

RESULTS AND DISCUSSION

Sizing aquatic bacteria involves the difficulty of dealing with very small cells, close to the limit of resolution of light microscopy. Under epifluorescence microscopy, bacteria appear as bright particles on a dark background, which complicates determination of their true edges. Researchers have developed ways to account for the halo effects (Sieracki *et al.*, 1989a; Schröder and Krambeck, 1991; Psenner, 1991; Bjørnsen *et al.*, 1995). However, there are also other problems encountered in daily practice. In this paper we present how we determine bacterial

volume in our laboratory, and how we optimized the process. We will separately analyze the different steps that can introduce variations in size determinations, such as the brightness of the captured image, the choice of the threshold level or the effect of the formula used to compute the bacterial volume. Then, we will calibrate our system against reference objects. Finally, we will discuss the statistically appropriate number of cells and images to be analyzed to minimize errors.

Differences in brightness of the captured images

Conventional cameras do not have enough sensitivity to detect the small and dim bacteria visualized by epifluorescence. This problem is solved either by photomultiplying the light signal or by increasing the exposure time during image capturing. Our camera (Hamamatsu C2400-08) follows the first strategy. The operator chooses the brightness of the image and, obviously, different operators can choose different levels. To test how variations in image brightness affected our determinations, we captured three images from the same microscopic field using three levels of exposure, one considered to be the optimal, and the others above and below this optimal level (Fig. 4). This was done six times and in all cases the average value obtained by the under- and overexposed image was statistically the same as the value obtained for the optimally-exposed image (t-tests, $P < 0.005$). We argue that most operators would
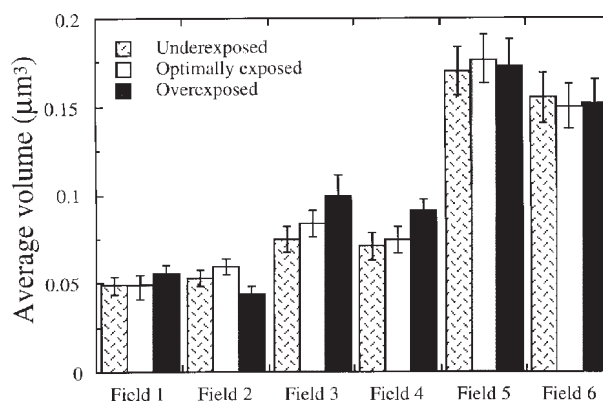

FIG. 4. – Average bacterial volume (±SE) obtained after measuring the same microscopic field captured at optimal brightness (optimally exposed) and above (overexposed) or below (underexposed) this optimal level.

choose a level close to the optimal, and in any case within the range represented by the lower and upper levels. This absence of difference, despite the widespread prejudice that brighter images will result in larger bacteria, is a demonstration of the power of the second derivative filter used during image processing.

Operator intervention in the image processing

The image processing proposed is semi-automatic, with two steps requiring operator intervention. The choice of the threshold level before binarizing

TABLE 2. – Variability among operators when estimating cell count and average bacterial volume. Five epifluorescence images were analyzed by 10 different operators. Data are presented as the measured value divided by the Among-Operator Average. Among-Operator Error (AO error) is computed as Standard error of interoperator estimates divided by Average value and is expressed as a percentage.

	Cell count (10^6 cells ml^{-1})						Average bacterial volume (μm^3)				
Operator	Image 1	Image 2	Image 3	Image 4	Image 5		Image 1	Image 2	Image 3	Image 4	Image 5
R	1.026	0.927	0.925	1.000	0.947		0.998	1.074	1.058	1.044	1.093
P	0.949	1.026	0.940	1.000	0.947		1.036	0.967	0.971	1.118	1.032
T	1.051	0.945	1.013	1.000	1.000		-	-	1.092	1.116	1.249
E	1.026	1.116	1.013	1.063	1.000		-	1.034	0.906	0.906	0.890
C	0.949	0.999	0.984	1.000	1.105		1.018	1.100	1.075	1.093	1.008
G	1.026	0.963	1.013	1.000	0.947		0.884	0.798	-	-	-
J	0.872	-	0.925	0.875	0.985		-	0.783	1.056	0.819	-
N	1.077	1.098	1.101	0.938	1.053		1.064	-	1.025	1.000	0.810
D	1.077	1.053	1.072	1.125	1.105		1.026	1.006	1.043	0.903	0.918
H	0.949	0.873	1.013	-	-		0.964	1.239	0.775	-	-
Average value	6.67	18.22	22.44	1.44	1.11		0.056	0.107	0.138	0.093	0.071
% AO error	2.1	2.7	1.9	2.3	2.5		2.3	5.3	3.4	4.0	5.5

the image is the most critical. This step is best accomplished by the zero-crossing technique, an automatic process that is also the most accurate (Sieracki *et al.*, 1989a). The image obtained after the application of the Laplace filter presents gray level values of 0 for the background, and a change from negative to positive values at the points of maximal gradient. Following the zero-crossing technique the threshold level is set to 1. Together with bacteria, many noise particles from the background are selected, and thus high-quality images and special algorithms to delete background noise are required. Here we describe a process that is almost equivalent to the zero-crossing technique. With the option "Scale Convolutions" in NIH-Image, the results of the Laplace filter are scaled, and the resultant gray value for the background is higher than 0 (i.e. 150). This allows to threshold at a slightly lower gray level (i.e. 148), and this avoids selecting most of the noise. Therefore, our procedure allows the processing of medium-quality images which could not be automatically analyzed with the zero-crossing technique.

To test the effect of the operator in image processing, five very different images were processed by ten operators (Table 2). The average values for cell count and cell volume were assumed to be the "true" values (Table 2). The table shows the values estimated by each operator divided by the averaged values. In this way, 75% and 88% of the estimates of volume and 86% and 100% of the cell counts were within the 10% and 20%, respectively, of the average values. The average error (as standard error of interoperator estimates divided by average value) ranged from 1.9 to 2.7% for cell counts, and from 2.3 to 5.5% for cell volumes (Table 2). Interoperator variability in analyzing the same image with our system was therefore 5% as a maximum.

Calculation of bacterial volume

As shown in Fig. 3, different algorithms can be used to calculate bacterial volume from the parameters provided by the image analysis software. An understanding of how the different parameters are obtained is necessary to discuss the use of each algorithm. One parameter, Area, is determined by counting the number of pixels of the binarized cell (Fig. 5A). The other three parameters are derived from the binarized cell by applying special algorithms that may be different in different software packages. NIH-Image calculates Length and Width as the major and minor axis of the best-fitting ellipse (Fig.
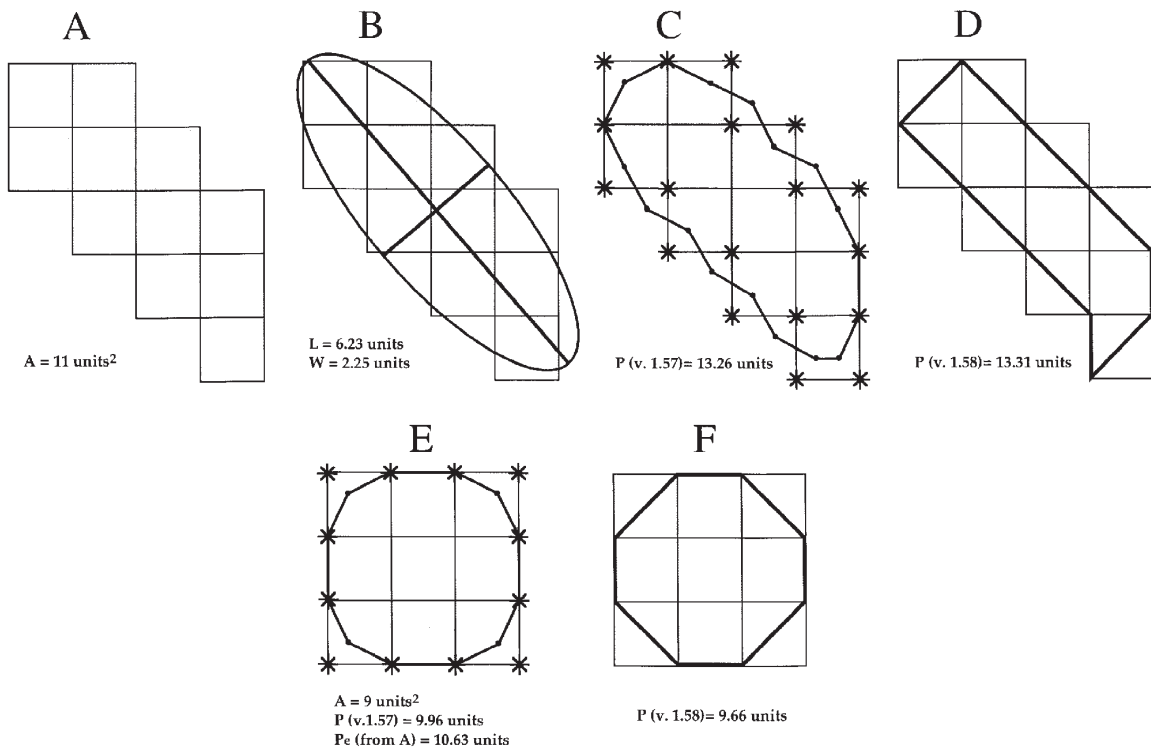

FIG. 5. – A-C: Representation of the way in which NIH-Image (v.1.57) computes A, L, W and P from the binarized image of a bacterium (see text for explanation). D: Calculation of the perimeter by the newer versions of NIH-Image (1.58 to 1.61). E-F: The insoluble geometrical problem produced by NIH-Image with very small bacteria. The perimeter calculated by NIH-Image (9.96 with v. 1.57; 9.66 with v. 1.58) is smaller than the minimal perimeter that closes the area measured (10.63).
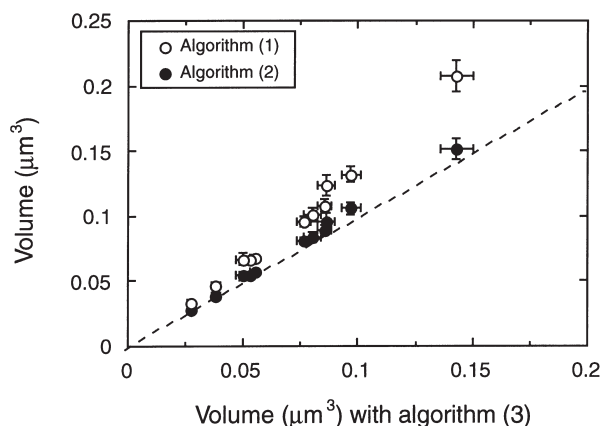
FIG. 6. – Comparison of the average bacterial volume (± SE) in a set of very different water systems, as computed with Algorithms 1, 2 and 3.
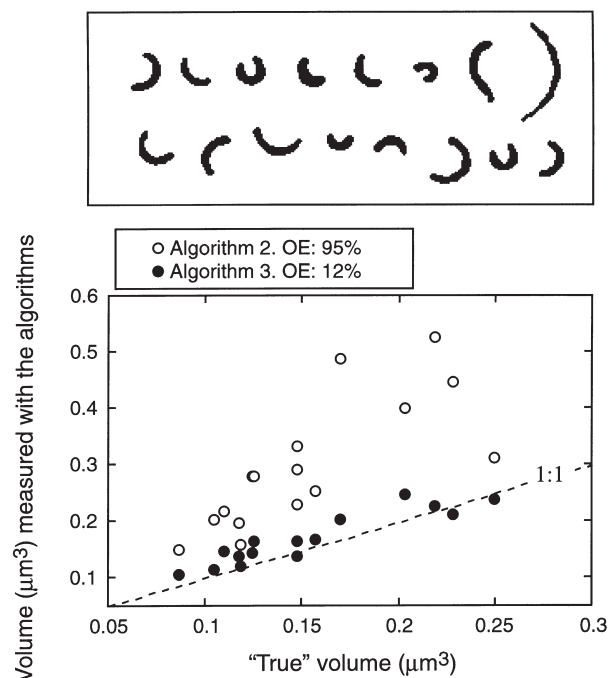

FIG. 7. – Comparison of the performance of Algorithms 2 and 3 to calculate the volume of curved bacteria. The cells in the upper panel were digitized from different natural samples. The length along its main axis and the width (at three sections) were measured manually and used to calculate the "True" volume. The cells were then treated by image analysis and their volume calculated with Algorithms 2 and 3. OE: Overestimation as % of true value.

5B). To calculate the Perimeter, NIH-Image (versions 1.53 to 1.57; here we used v. 1.57) determines the coordinates of the cell (stars in Fig. 5C) and finds new coordinates (points in Fig. 5C) averaging the position of the three nearest coordinates. The Perimeter is then calculated as the sum of the distances between these new coordinates (Fig. 5C). Newer versions of NIH-Image (1.58 to 1.61) apply a different formula, which adds 1 to the perimeter for each edge pixel and the square root of 2 for each corner pixel (Fig. 5D), and produces perimeters slightly smaller than that previously described (average of 2.1% in 111 cells analyzed).

The simplest algorithm (Algorithm 1, Fig. 3) uses L and W directly as provided by the software. This could cause some inaccuracies since the model used to estimate L and W (ellipse, Fig. 5B), is different from the model to calculate volume (cylinder with two hemispherical caps). Of the two, W is the most sensitive parameter, since W is considerably larger in an ellipse than in a cylinder. Algorithm 2 reduces this problem by using the equivalent width (W_e, Eq. 2), calculated from A and L. Algorithm 3 makes a further step and uses equivalent width (W_e, Eq. 4) and equivalent length (L_e, Eq. 5), calculated from A and P.

As expected, Algorithms 2 and 3 performed similarly for a variety of field samples (Fig. 6), unlike Algorithm 1, which overestimated bacterial volume in most instances. In addition, Algorithm 3 was clearly superior when analyzing curved rods or filaments (Fig. 7), since estimation of L with the best fitting ellipse model resulted in a large error in these cases. We assembled an image with curved bacteria from different natural samples, manually measured their

length and width and calculated their volume (the "true" volume). We then applied both Algorithms 2 and 3 to estimate the volumes. Algorithm 3 overestimated volume very slightly, while Algorithm 2 greatly overestimated the volume of these cells (Fig. 7).

Therefore, we decided to routinely use Algorithm 3. A problem appeared, however, when using this algorithm with NIH-Image and some other software packages (such as OptiLab). In some very small cocci the area did not fit into the calculated perimeter (see Figs. 5E and 5F). This fact, caused by the way in which the perimeter is calculated, is geometrically impossible and results in a square root of a negative number in Eq. 4. (This problem occurs in more cells with newer versions of NIH-Image). For such cells, we suggest to use Eq. 7 which calculates the volume assuming the cell to be a sphere, and thus using only A. We have analyzed the effect of Eq. 7 for a set of cells, typically of less than 20 or 30 pixels in area, that presented this problem. The use of Eq. 7 overestimated the volume (as compared to the volume calculated with Algorithm 2) by 8.5% on average (N = 11), with cells ranging from 0.004 to 0.042 μm^3. This very slight overestimation does not affect the estimation of average bacterial volume significantly.

Bacterial counts by image analysis

The image analysis of bacteria is not aimed at counting bacteria, since the routine manual count is easy and does not consume much time. In addition, the area to be digitized is not selected at random, but instead, fields with a high number of cells and lack of bright particles or aggregates are chosen. However, when we compared the bacterial numbers obtained by manual counts and through image analysis (considering the number of cells measured and the number of images processed), we found a very good agreement (Fig. 8). Therefore, simultaneously with bacterial volumes, the described image analysis system provides a very good estimate of bacterial abundance.

System calibration

Calibration of the system was done by comparing estimates of the sizes of fluorescent beads against the nominal sizes reported by the manufacturers. We used Polysciences Fluoresbrite latex beads of 0.51, 0.74 and 2.44 μm in diameter. The smallest beads are close to the size of most bacteria in nature, only slightly larger than most marine bacteria. The second type of beads are at the highest end of the size range encountered in nature and they are similar to the sizes of many cultured bacteria. We also used 2.44 μm beads to see how well did our system perform in the size range of nanoplankton. Our system produced a small overestimation of bead area (3 - 8%, Table 3) and a small underestimation of bead volume (4 - 13%) in the relevant size range. Outside of this size range, our system underestimated bead volume (30%) although underestimation of bead area was relatively small (7%). These values are very reasonable and similar to those found by others (Bjørnsen, 1986; Schröder and Krambeck, 1991; Bloem *et al.*, 1995).
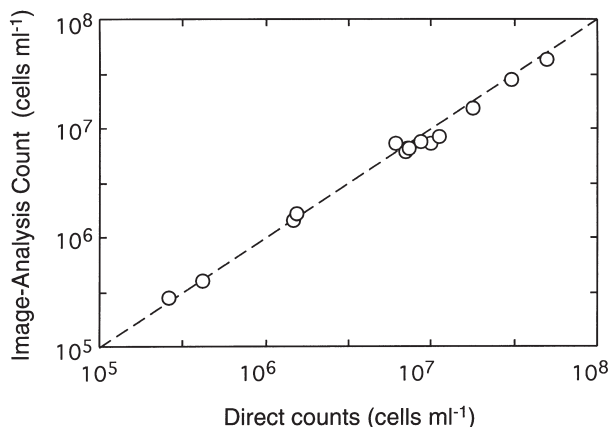

FIG. 8. – Comparison of bacterial abundance as obtained by direct epifluorescence counts and automatically by image analysis. Samples from different water bodies.

Optimal number of images and cells to be analyzed per sample

The more cells analyzed, the better the estimate of average bacterial size. However, the relationship between number of cells (or images) analyzed and error is not linear. From a certain point on, many more cells have to be measured to decrease the error by a certain percentage. To estimate the number of cells that should be enough for minimizing the value of variability (error) while simultaneously minimizing the sample treatment time, we calculated the average volume and its standard error (SE) after considering an increasing number of cells from the same sample (Figs. 9A, 9C and 9E). Figs. 9B, 9D and 9E show the average volumes and their SE when increasing the number of images considered. In the three cases analyzed the average volume was fairly constant after 170 cells had been measured

TABLE 3. – Calibration of the image analysis system against fluorescent latex beads of known size. SE shown between parenthesis. OE: Overestimation as % of nominal value.

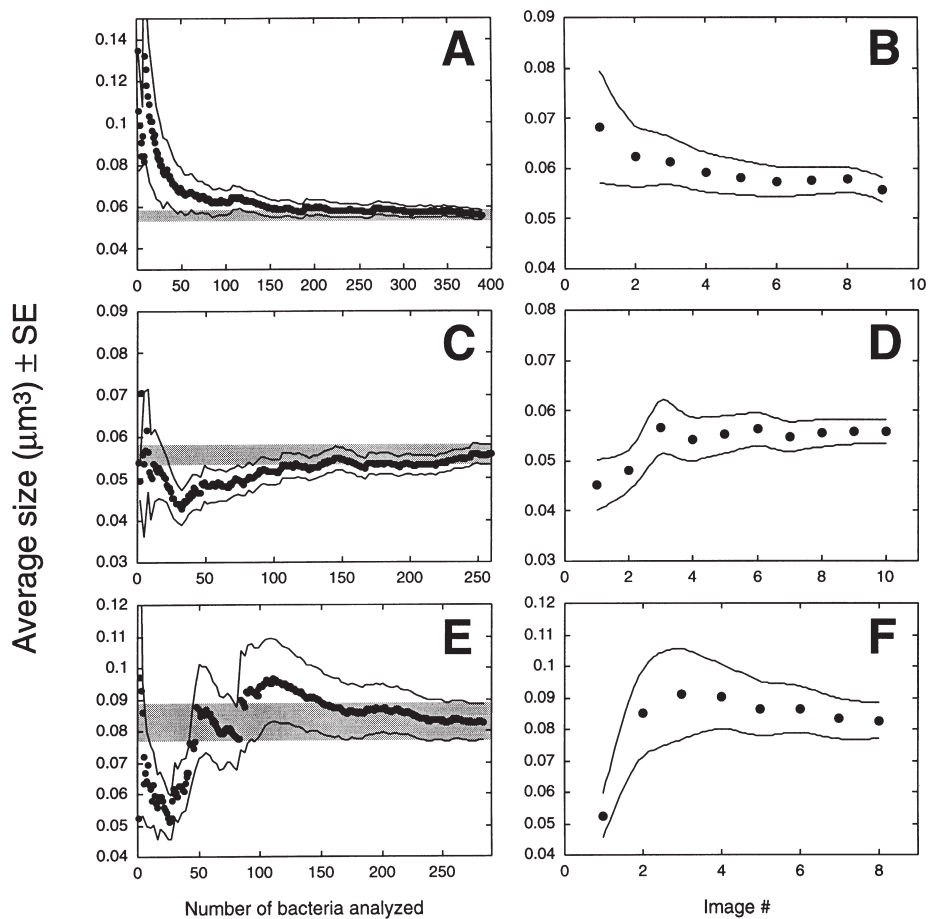| Particle	Area (μm²)			Volume (μm³)		
diameter	Nominal	Measured	OE	Nominal	Measured	OE
0.51 μm	0.204	0.221 (0.002)	8.3	0.069	0.066 (0.001)	-4.3
0.74 μm	0.430	0.443 (0.004)	3.0	0.212	0.184 (0.002)	-13.2
2.44 μm	4.676	4.361 (0.038)	-6.7	7.606	5.257 (0.086)	-30.1

FIG. 9. – A-C-E: Change in average bacterial volume (filled circles) and its Standard Error (upper and lower lines) after averaging a different number of cells in three different samples. The gray area in the graphs correspond to the final average volume (± SE) in each sample. Panels on the right (B-D-F) correspond to the same data sets as the left panels, averaging the results of one, two or more images analyzed from the same sample.

and after four to five images had been treated. In addition, the error did not decrease significantly when more cells or images were treated. In conclusion, 200 - 250 cells in 4 to 6 images are the ideal values to obtain a good estimate of bacterial average size, with minimal variability and with the least possible time consumed. An amount of 40-50 cells per image is also good for having them spread out in the filter without too many falling one on top of the other.

ACKNOWLEDGMENTS

REFERENCES

Alldredge, A.L., J.J. Cole and D.A. Caron. - 1986. Production of heterotrophic bacteria inhabiting macroscopic organic aggregates (marine snow) from surface waters. *Limnol. Oceanogr.* 31: 68-78.

Billen, G., P. Servais and S. Becquevort. – 1990. Dynamics of bacterioplankton in oligotrophic and eutrophic aquatic environments: bottom-up or top-down control? *Hydrobiologia* 207: 37-42.

Bjørnsen, P.K. – 1986. Automatic determination of bacterioplankton biomass by image analysis. *Appl. Environ. Microbiol.* 51: 1199-1204.

Bjørnsen, P.K., B. Riemann, J. Pock-Steen, T.G. Nielsen and S.J. Horsted. – 1989. Regulation of bacterioplankton production and cell volume in a eutrophic estuary. *Appl. Environ. Microbiol.* 55: 1512-1518.

Bjørnsen, P.K., Å. Hagström, B. Hygum, T.G. Nielsen, N. Blackburn, R. Massana, C. Pedrós-Alió, C. Svarer, L.K. Hansen, S. Hietanen and J. Kuparinen. – 1995. DIADEME: Digital Image Analysis Development in European Marine Ecology. Scientific Report of the Contract No. MAS2-CT93-0077.

Bloem, J., M. Veninga and J. Shepherd. – 1995. Fully automatic determination of soil bacterium numbers, cell volumes, and frequencies of dividing cells by confocal laser scanning microscopy and image analysis. *Appl. Environ. Microbiol.* 61: 926-936.

Chrzanowski, T.H., R.D. Crotty and G.J. Hubbard. – 1987. Seasonal variation in cell volume of epilimnetic bacteria. *Microb. Ecol.* 16: 155-163.

Cole, J.J., M.L. Pace, N.F. Caraco and G.S. Steinhart. – 1993. Bacterial biomass and cell size distributions in lakes: More and larger cells in anoxic waters. *Limnol. Oceanogr.* 38: 1627-1632.

del Giorgio, P.A., D.F. Bird, Y.T. Prairie and D. Planas. – 1996. The flow cytometric determination of bacterial abundance in lake plankton using the green nucleic acid stain SYTO 13. *Limnol. Oceanogr.* 41: 783-789.

Estep, K.W., F. MacIntyre, E. Hjörleifsson and J.McN. Sieburth. – 1986. MacImage: a user-friendly image-analysis system for the accurate mensuration of marine organisms. *Mar. Ecol. Prog. Ser.* 33: 243-253.

Fry, J.C. – 1990. Direct methods and biomass estimation. *Meth. Microbiol.* 22: 41-85.

Fuhrman, J.A. – 1981. Influence of methods on the apparent size distribution of bacterioplankton cells: epifluorescence microscopy compared to scanning electron microscopy. *Mar. Ecol. Prog. Ser.* 5: 103-106.

Gasol, J.M., P.A. del Giorgio, R. Massana and C.M. Duarte. – 1995. Active versus inactive bacteria: size-dependence in a coastal marine plankton community. *Mar. Ecol. Progr. Ser.* 128: 91-97.

Gasol, J.M., R. Massana and C. Pedrós-Alió. – in press. Bacterial size structure as a method to analyze communities. In: *Proceedings of the Seventh International Symposium of Microbial Ecology*, Brazilian Soc. Microbiol., Santos, Brazil.

Hygum, B.H. – 1995. Abundance, volume and distribution of bacterioplankton and sub-micron particles in the open Baltic Sea. Proc. Sixth Int. Work. Meas. Microb. Act. Cycl. Matter in Aquat. Envir., Konstanz, Germany.

Jürgens, K. and H. Güde. – 1994. The potential importance of grazing-resistant bacteria in planktonic systems. *Mar. Ecol. Prog. Ser.* 112: 169-188.

Krambeck, C., H.-J. Krambeck, D. Schröder and S.Y. Newell. – 1990. Sizing bacterioplankton: a juxtaposition of bias due to shrinkage, halos, subjectivity in image interpretation and asymmetric distributions. *Binary* 2: 5-14.

Lee, S.H., Y.-C. Kang and J.A. Fuhrman. – 1995. Imperfect retention of natural bacterioplankton cells by glass fiber filters. *Mar. Ecol. Prog. Ser.* 119: 285-290.

Li, W.K.W., J.F. Jellett and P.M. Dickie. – 1995. DNA distributions in planktonic bacteria stained with TOTO or TO-PRO. *Limnol. Oceanogr.* 40: 1485-1495.

Novitsky, J.A. and R.Y. Morita. – 1976. Morphological characterization of small cells resulting from nutrient starvation of a psychrophilic marine vibrio. *Appl. Environ. Microbiol.* 32: 617-622.

Peters, R.H. – 1983. The ecological implications of body size. Cambridge Univ. Press, Cambridge, Massachusetts, USA.

Porter, K.G. and Y.S. Feig. – 1980. The use of DAPI for identification and enumeration of aquatic microflora. *Limnol. Oceanogr.* 25: 943-948.

Psenner, R. – 1991. Determination of bacterial cell volumes by image analysis. *Verh. Internat. verein. Limnol.* 24: 2605-2608.

Psenner, R. – 1993. Determination of size and morphology of aquatic bacteria by automated image analysis. In: P.F. Kemp, B.F. Sherr, E.B. Sherr and J.J. Cole (Eds.): *Handbook of Methods in Aquatic Microbial Ecology*, pp. 339-345. Lewis Publ., Boca Raton, Florida, USA.

Robertson, B.R. and D.K. Button. – 1989. Characterizing aquatic bacteria according to population, cell size, and apparent DNA content by flow cytometry. *Cytometry* 10: 70-76.

Schröder, D. and H.-J. Krambeck. – 1991. Advances in digital image analysis of bacterioplankton with epifluorescence microscopy. *Verh. Internat. verein. Limnol.* 24: 2601-2604.

Sieracki, M.E., P.W. Johnson and J.McN. Sieburth. – 1985. Detection, enumeration and sizing of planktonic bacteria by image-analysed epifluorescence microscopy. *Appl. Environ. Microbiol.* 49: 799-810.

Sieracki, M.E., S.E. Reichenbach and K.L. Webb. – 1989a. Evaluation of automated threshold selection methods for accurately sizing microscopic fluorescent cells by image analysis. *Appl. Environ. Microbiol.* 55: 2762-2772.

Sieracki, M.E., C.L. Viles and K.L. Webb. – 1989b. Algorithm to estimate cell biovolume using image analyzed microscopy. *Cytometry* 10: 551-557.

Sieracki, M.E. and K.L. Webb. – 1991. The application of image-analyzed fluorescence microscopy for characterizing planktonic bacteria and protists. In: P.C. Reid, C.M. Turley and P.H. Burkill (Eds.): *Protozoa and their role in marine processes*, pp. 77-100. NATO ASI Ser. vol. 25, Springer Verlag, Berlin.

Sieracki, M.E., E.M. Haugen and T.L. Cucci. – 1995. Overestimation of heterotrophic bacteria in the Sargasso Sea: direct evidence by flow and imaging cytometry. *Deep-Sea Res.* 42: 1399-1409.

Sommaruga, R. and R. Psenner. – 1995. Permanent presence of grazing-resistant bacteria in a hypertrophic lake. *Appl. Environ. Microbiol.* 61: 3457-3459.

Verity, P.G. and M.E. Sieracki. – 1993. Use of color image analysis and epifluorescence microscopy to measure plankton biomass. In: P.F. Kemp, B.F. Sherr, E.B. Sherr and J.J. Cole (Eds.): *Handbook of Methods in Aquatic Microbial Ecology*, pp. 327-338. Lewis Publ., Boca Raton, Florida, USA.

Viles, C.L. and M.E. Sieracki. – 1992. Measurement of marine picoplankton cell size by using a cooled, charge-coupled device camera with image-analyzed fluorescence microscopy. *Appl. Environ. Microbiol.* 58: 584-592.

White, P.A., J. Kalff, J.B. Rasmussen and J.M. Gasol. – 1991. The effect of temperature and algal biomass on bacterial production and specific growth rate in freshwater and marine habitats. *Microb. Ecol.* 21: 99-118.

Scient. ed.: R. Guerrero